

## Preparation, Crystal Structures and Spectroscopic Properties of a Series of Cobalt(III) Phosphine Complexes: *trans*- and *cis*-[Co(dtc)<sub>2</sub>(PMe<sub>3-n</sub>Ph<sub>n</sub>)<sub>2</sub>]<sup>+</sup> (dtc = *N,N*-Dimethyldithiocarbamate; *n* = 0, 1, 2 or 3)

Takayoshi Suzuki,\* Shinsaku Kashiwamura,<sup>†</sup> and Kazuo Kashiwabara\*<sup>,†</sup>

Department of Chemistry, Graduate School of Science, Osaka University, Toyonaka 560-0043.

<sup>†</sup>Department of Chemistry, Graduate School of Science, Nagoya University, Chikusa-ku, Nagoya 464-8602.

(Received June 22, 2001)

A series of new cobalt(III) phosphine complexes of *trans*-[Co(dtc)<sub>2</sub>(PMe<sub>3-n</sub>Ph<sub>n</sub>)<sub>2</sub>]BF<sub>4</sub> (dtc = *N,N*-dimethyldithiocarbamate; *n* = 0, 1, 2 or 3) and *cis*-[Co(dtc)<sub>2</sub>(PMe<sub>3</sub> or PMe<sub>2</sub>Ph)<sub>2</sub>](BF<sub>4</sub> or PF<sub>6</sub>) have been prepared and their crystal structures and spectroscopic properties have been investigated. It is found that the Co–S bond lengths vary with steric and electronic factors of the P-ligands; i.e. (1) the intramolecular  $\pi$ – $\pi$  stacking interaction between the dtc plane and the phenyl ring of the P-ligand, and (2) the electronic *trans* influence of the *trans*-positioned P-ligand. The strength of electronic *trans* influence decreases as PMe<sub>3</sub> > PMe<sub>2</sub>Ph > P(OCH<sub>2</sub>)<sub>3</sub>CEt in accordance with the order of  $\sigma$ -donicity strengths. In the series of *trans*-isomers, the electronic *trans* influence is competitive with the steric requirement of the phosphine to elongate the mutually *trans* Co–P bonds. The steric *trans* influence via the equatorial dtc ligands for such an elongation of the Co–P bonds seems to be negligible, which is in sharp contrast to the situation for via pentane-2,4-dionate (acac) ligands in the analogous complexes, *trans*-[Co(acac)<sub>2</sub>(PMe<sub>3-n</sub>Ph<sub>n</sub>)<sub>2</sub>]PF<sub>6</sub>. This is probably due to the compactness of dtc and the resulting open space at the Co atom. The fact that the Co–P bond lengths in the dtc complexes are shorter than those in the acac complexes is reflected in the larger stability toward hydrolysis of the dtc complexes. In the UV-vis absorption spectra, the degenerate splitting component (<sup>1</sup>E<sub>g</sub>) of the first d–d transition band of *trans*-[Co(dtc)<sub>2</sub>(PMe<sub>3-n</sub>Ph<sub>n</sub>)<sub>2</sub>]<sup>+</sup> is observed at almost the same position (within 300 cm<sup>-1</sup>) as that of the corresponding acac complexes, while the transition energies of the P-to-Co LMCT of these two series of complexes are rather different (at least 2700 cm<sup>-1</sup>) from each other. Furthermore, the first and the second d–d transition bands of *cis*-[Co(dtc)<sub>2</sub>(PMe<sub>3</sub> or PMe<sub>2</sub>Ph)<sub>2</sub>]<sup>+</sup> are observed at lower energy than those of *cis*-[Co(dtc)<sub>2</sub>{P(OMe)<sub>3</sub>}]<sup>+</sup> in spite of a weaker  $\sigma$ -donor of phosphite. The separation of the first and the second d–d transition bands of the P(OMe)<sub>3</sub> complex is remarkably smaller than the separation of the bands of the PMe<sub>3</sub> one, being indicative of a further reduction of the interelectronic repulsion in the P(OMe)<sub>3</sub> complex.

In previous studies,<sup>1–8</sup> we have prepared several series of mixed-ligand phosphine complexes of cobalt(III) with pentane-2,4-dionate (acac) and investigated their crystal and molecular structures, spectroscopic and electrochemical properties, and reactivities toward isomerization or hydrolysis. While oxidation of an ethanolic mixture of [Co(acac)<sub>2</sub>(H<sub>2</sub>O)<sub>2</sub>] and PPh<sub>3</sub> with PbO<sub>2</sub>/AcOH yielded *trans*-[Co(acac)<sub>2</sub>(PPh<sub>3</sub>)<sub>2</sub>]<sup>+</sup> exclusively, a similar reaction using PMe<sub>3</sub> afforded only *cis*-isomer.<sup>4</sup> Such a difference in the preference of a particular geometrical isomer would result from competition between electronic and steric requirements of phosphines; strong Lewis bases such as PMe<sub>3</sub> tend to form a mutually *cis* configuration, which is unfavorable for bulky phosphines like PPh<sub>3</sub>. However, *trans*-[Co(acac)<sub>2</sub>(PMe<sub>3</sub>)<sub>2</sub>]<sup>+</sup> was synthesized by a reaction of PMe<sub>3</sub> with *trans*-[Co(acac)<sub>2</sub>(PPh<sub>3</sub>)<sub>2</sub>]<sup>+</sup> in methanol.<sup>2</sup> Once isolated, the *trans*-isomer is stable toward isomerization in dry organic solvents, but readily hydrolyzed in wet organic solvents to form *trans*-[Co(acac)<sub>2</sub>(PMe<sub>3</sub>)(H<sub>2</sub>O)]<sup>+</sup>, while the *cis*-[Co(acac)<sub>2</sub>(PMe<sub>3</sub>)<sub>2</sub>]<sup>+</sup> is stable toward isomerization and hydrolysis in the same condition.<sup>2,4</sup> In order to interpret these properties of the mixed-ligand acac–phosphine complexes from structural points of view, we performed the X-ray crystal structure analy-

ses for several series of complexes,<sup>1–3,6,8</sup> and found that the differences in Co–P bond lengths are closely correlated to these properties. For example, the strong electronic *trans* influence of PMe<sub>3</sub>, which was indicated by comparison of the Co–O bond lengths between *cis*- and *trans*-[Co(acac)<sub>2</sub>(PMe<sub>3</sub>)<sub>2</sub>]<sup>+</sup>, gave mutual large elongation of Co–P bonds in the *trans*-isomer.<sup>2</sup> In addition, the steric *trans* influence of PPh<sub>3</sub> was realized from the structural analysis of *trans*-[Co(acac)<sub>2</sub>(PPh<sub>3</sub>)<sub>2</sub>]<sup>+</sup>.<sup>1</sup> These electronic and steric *trans* influences of phosphines would lead to high reactivities of the *trans*-isomers for substitution and/or hydrolysis.

We have also prepared a number of mixed-ligand *N,N*-dimethyldithiocarbamate (dtc) complexes of cobalt(III) incorporating phosphines, phosphinites, phosphonites, or phosphites (P-ligand).<sup>8–14</sup> In the case of monodentate phosphite (P(OMe)<sub>3</sub>, P(OEt)<sub>3</sub>, P(OCH<sub>2</sub>)<sub>3</sub>CEt), the *cis*-isomers of [Co(dtc)<sub>2</sub>(phosphite)]<sup>+</sup> were readily converted photochemically to the *trans*-isomers, which isomerized thermally to the original *cis*-isomers.<sup>10,13</sup> From these previous findings, we concluded that it would be interesting to prepare a series of mixed-ligand dtc–monodentate phosphine complexes: [Co(dtc)<sub>2</sub>(PMe<sub>3-n</sub>Ph<sub>n</sub>)<sub>2</sub>]<sup>+</sup> (*n* = 0, 1, 2 or 3), and to compare their molecular structures

and chemical and spectroscopic properties to those of the related complexes above. However, there were only two complexes so far for the monodentate phosphines: *trans*-[Co(*dtc*)<sub>2</sub>(PPh<sub>3</sub> or PEt<sub>3</sub>)<sub>2</sub>]<sup>+</sup>.<sup>9</sup> Here, we will describe preparation, X-ray structural analyses and spectroscopic characterization of *trans*-[Co(*dtc*)<sub>2</sub>(PMe<sub>3</sub>)<sub>2</sub>]BF<sub>4</sub> (***t*-0**), *trans*-[Co(*dtc*)<sub>2</sub>(PMe<sub>2</sub>Ph)<sub>2</sub>]BF<sub>4</sub> (***t*-1**), *trans*-[Co(*dtc*)<sub>2</sub>(PMePh<sub>2</sub>)<sub>2</sub>]BF<sub>4</sub> (***t*-2**), *trans*-[Co(*dtc*)<sub>2</sub>(PPh<sub>3</sub>)<sub>2</sub>]BF<sub>4</sub> (***t*-3**), *cis*-[Co(*dtc*)<sub>2</sub>(PMe<sub>3</sub>)<sub>2</sub>]BF<sub>4</sub> (***c*-0**), and *cis*-[Co(*dtc*)<sub>2</sub>(PMe<sub>2</sub>Ph)<sub>2</sub>]PF<sub>6</sub> (***c*-1'**).

### Experimental

Phosphines were handled under an atmosphere of argon until such time as they formed air-stable cobalt(III) complexes. All of the solvents used in the preparation of complexes were deaerated with argon for 20 min immediately before use. [Co(*dtc*)<sub>3</sub>] was prepared by the literature method<sup>15</sup> and recrystallized from dichloromethane and methanol.

***trans*-[Co(*dtc*)<sub>2</sub>(PPh<sub>3</sub>)<sub>2</sub>]BF<sub>4</sub> (***t*-3**):** In order to achieve a higher yield and a better purity of this complex, the previous method<sup>9</sup> was modified as follows. To a pink-colored ethanolic solution (200 cm<sup>3</sup>) containing Co(BF<sub>4</sub>)<sub>2</sub>·6H<sub>2</sub>O (2.01 g, 5.90 mmol) and PPh<sub>3</sub> (3.11 g, 11.8 mmol) was added a pale yellow solution of tetramethylthiuram disulfide (1.41 g, 5.86 mmol) in a mixture of dichloromethane and ethanol (1:1, 60 cm<sup>3</sup>) with stirring. The mixture was stirred for 1 h at room temperature, and a brown precipitate which formed was collected by filtration. To remove a by-product of [Co(*dtc*)<sub>3</sub>], the product was dissolved in dichloromethane (30 cm<sup>3</sup>) and reprecipitated by addition of diethyl ether (70 cm<sup>3</sup>). The precipitate was filtered off, and dissolved in a mixture of dichloromethane and ethanol (1:1, 140 cm<sup>3</sup>). Slow evaporation of the solution to ca. 60 cm<sup>3</sup> in the open air afforded brown needle crystals of ***t*-3**. Yield: 2.42 g (45.0%). Purple hexagonal plate crystals of ***t*-3**·H<sub>2</sub>O suitable for X-ray analysis were obtained by repeated recrystallization from CH<sub>2</sub>Cl<sub>2</sub>/CH<sub>3</sub>OH in the open air. Anal. Found: C, 54.22; H, 4.66; N, 3.08%. Calcd for C<sub>42</sub>H<sub>44</sub>BCoF<sub>4</sub>N<sub>2</sub>OP<sub>2</sub>S<sub>4</sub>: C, 54.32; H, 4.78; N, 3.02%.

***trans*-[Co(*dtc*)<sub>2</sub>(PMePh<sub>2</sub>)<sub>2</sub>]BF<sub>4</sub> (***t*-2**):** To a pink-colored methanol solution (80 cm<sup>3</sup>) of Co(BF<sub>4</sub>)<sub>2</sub>·6H<sub>2</sub>O (977 mg, 2.87 mmol) was added PMePh<sub>2</sub> (1.15 g, 5.74 mmol) with stirring; the color of the mixture turned to orange immediately. A solution of tetramethylthiuram disulfide (689 mg, 2.87 mmol) in a mixture of dichloromethane and methanol (1:2, 60 cm<sup>3</sup>) was added with stirring to the orange solution, and the mixture was stirred for 2 h at room temperature. The reaction mixture was then filtered to remove a green precipitate of [Co(*dtc*)<sub>3</sub>]. The filtrate was concentrated nearly to dryness under reduced pressure, and the residue was washed with diethyl ether (50 cm<sup>3</sup>). This crude product was found to be a mixture of ***t*-2** (ca. 92%), *cis*-[Co(*dtc*)<sub>2</sub>(PMePh<sub>2</sub>)<sub>2</sub>]BF<sub>4</sub> (***c*-2**: ca. 5%) and [Co(*dtc*)<sub>3</sub>] (ca. 3%) by <sup>1</sup>H NMR. The crude product was dissolved in hot methanol (60 °C, 70 cm<sup>3</sup>), and the filtered solution was cooled in a refrigerator overnight to give dark red needle crystals, which were collected by filtration and dried in air. The product was recrystallized from CH<sub>2</sub>Cl<sub>2</sub>/CH<sub>3</sub>OH, affording dark red columnar crystals of pure ***t*-2**. Yield: 1.35 g (59.9%). Anal. Found: C, 48.85; H, 4.81; N, 3.56%. Calcd for C<sub>32</sub>H<sub>38</sub>BCoF<sub>4</sub>N<sub>2</sub>P<sub>2</sub>S<sub>4</sub>: C, 48.86; H, 4.87; N, 3.56%.

***trans*-[Co(*dtc*)<sub>2</sub>(PMe<sub>2</sub>Ph)<sub>2</sub>]BF<sub>4</sub> (***t*-1**) and *cis*-[Co(*dtc*)<sub>2</sub>(PMe<sub>2</sub>Ph)<sub>2</sub>]PF<sub>6</sub> (***c*-1'**):** To a greenish brown methanol solution (50 cm<sup>3</sup>) containing Co(BF<sub>4</sub>)<sub>2</sub>·6H<sub>2</sub>O (1.48 g, 4.36 mmol) and PMe<sub>2</sub>Ph (1.20 g, 8.69 mmol) was added a solution of tetramethylthiuram disulfide (1.05 g, 4.36 mmol) in a mixture of dichloromethane and

methanol (1:1, 40 cm<sup>3</sup>) with stirring. The mixture was stirred for 2 h at room temperature, and the resulting brown solution was filtered to remove a green precipitate of [Co(*dtc*)<sub>3</sub>]. The filtrate was evaporated to dryness under reduced pressure. The residue was washed with diethyl ether (50 cm<sup>3</sup>), and then dissolved in a mixture of methanol and dichloromethane (10:1, 55 cm<sup>3</sup>). The filtered solution was divided into three portions, and each portion was placed on a column of Sephadex LH-20 (φ 4.5 × 40 cm). The adsorbed products were eluted with methanol, separating into four colored bands: the first, a minor brown band; the second, a major red purple band; the third, a minor yellow brown band; the fourth, a minor green band. The major red purple band was collected, and evaporated to dryness under reduced pressure. This residue was found to be a mixture of ***t*-1** (42%) and *cis*-[Co(*dtc*)<sub>2</sub>(PMe<sub>2</sub>Ph)<sub>2</sub>]BF<sub>4</sub> (***c*-1**: 58%) by <sup>1</sup>H NMR. In order to separate the isomers, the residue was dissolved in a mixture of methanol and dichloromethane (4:1, 50 cm<sup>3</sup>), the filtered solution was evaporated (to 30 cm<sup>3</sup>) in the open air, and the concentrate was cooled in a refrigerator overnight. Red brown needle crystals of pure ***t*-1** were deposited, which were collected by filtration and dried in air. The product was recrystallized from CH<sub>2</sub>Cl<sub>2</sub>/CH<sub>3</sub>OH to give dark red columnar crystals. Yield: 512 mg (17.7%). Anal. Found: C, 39.75; H, 5.17; N, 4.23%. Calcd for C<sub>22</sub>H<sub>34</sub>BCoF<sub>4</sub>N<sub>2</sub>P<sub>2</sub>S<sub>4</sub>: C, 39.89; H, 5.17; N, 4.23%.

From the filtrate of red brown needle crystals of ***t*-1**, crystals of the pure *cis*-isomer was obtained as the PF<sub>6</sub><sup>-</sup> salt (***c*-1'**) as follows. Solid NH<sub>4</sub>PF<sub>6</sub> (4.5 g) was added to the filtrate with stirring and the mixture was stirred for a while, to result in a red brown precipitate. The precipitate was collected by filtration, dried in vacuo, and dissolved in dichloromethane (10 cm<sup>3</sup>). To the filtered solution was diffused diethyl ether vapor in a closed vessel; the red plate crystals which deposited were collected by filtration. The product was recrystallized from CH<sub>2</sub>Cl<sub>2</sub>/CH<sub>3</sub>OH. Yield: 1.17 g (37.1%). Anal. Found: C, 36.65; H, 4.70; N, 3.92%. Calcd for C<sub>22</sub>H<sub>34</sub>CoF<sub>6</sub>N<sub>2</sub>P<sub>3</sub>S<sub>4</sub>: C, 36.67; H, 4.76; N, 3.89%.

***trans*-[Co(*dtc*)<sub>2</sub>(PMe<sub>3</sub>)<sub>2</sub>]BF<sub>4</sub> (***t*-0**):** To a suspension of complex ***t*-3** (1.37 g, 1.50 mmol) in methanol (100 cm<sup>3</sup>) was added a toluene solution of PMe<sub>3</sub> (1.0 mol dm<sup>-3</sup>, 3.0 cm<sup>3</sup>) with stirring. The mixture was stirred for 1 h at room temperature, giving a dark red solution. The solution was evaporated to dryness under reduced pressure, and the residue was thoroughly washed with diethyl ether (200 cm<sup>3</sup>). The product was found to be pure ***t*-0** by <sup>1</sup>H NMR. Yield: 723 mg (93.7%). Further purification was done by recrystallization from CH<sub>3</sub>OH to give red columnar crystals. Anal. Found: C, 26.70; H, 5.66; N, 5.18%. Calcd for C<sub>12</sub>H<sub>30</sub>BCoF<sub>4</sub>N<sub>2</sub>P<sub>2</sub>S<sub>4</sub>: C, 26.77; H, 5.62; N, 5.20%.

***cis*-[Co(*dtc*)<sub>2</sub>(PMe<sub>3</sub>)<sub>2</sub>]BF<sub>4</sub> (***c*-0**), *trans*-[Co(*dtc*)<sub>2</sub>(PMe<sub>3</sub>)<sub>2</sub>]PF<sub>6</sub> (***t*-0'**) and *cis*-[Co(*dtc*)<sub>2</sub>(PMe<sub>3</sub>)<sub>2</sub>]PF<sub>6</sub> (***c*-0'**):** To a methanol solution (70 cm<sup>3</sup>) of Co(BF<sub>4</sub>)<sub>2</sub>·6H<sub>2</sub>O (1.02 g, 3.00 mmol) was added a toluene solution of PMe<sub>3</sub> (1.0 mol dm<sup>-3</sup>, 6.0 cm<sup>3</sup>) with stirring; the color of the solution turned to green immediately. A solution of tetramethylthiuram disulfide (726 mg, 3.02 mmol) in a mixture of dichloromethane and methanol (1:1, 40 cm<sup>3</sup>) was added with stirring to the green solution. After stirring for 2 h at room temperature, the mixture was evaporated to dryness under reduced pressure. The residue was washed with diethyl ether (100 cm<sup>3</sup>), and dissolved in methanol (40 cm<sup>3</sup>). Undissolved green precipitate was filtered off, and the filtrate was again evaporated to dryness under reduced pressure. The residue was dissolved in a mixture of methanol and dichloromethane (4:1, 20 cm<sup>3</sup>), and the filtered solution was placed on a column of Sephadex LH-20 (φ 4.5 × 40 cm). The adsorbed products were eluted with methanol,

separating into four colored bands: the first, a major red purple band; the second, a minor brown band; the third, a minor green band; the fourth, a minor pink band. The major red purple band was collected, and evaporated to dryness under reduced pressure. This residue was found to be a mixture of **t-0** (35%) and **c-0** (65%) by  $^1\text{H}$  NMR. In order to separate the isomers, the residue was dissolved in hot methanol (50 °C, 15 cm<sup>3</sup>), and the filtered solution was slowly cooled to room temperature to form red prismatic crystals of **c-0**. Further purification was done by recrystallization from  $\text{CH}_2\text{Cl}_2/\text{CH}_3\text{OH}$ . Yield: 315 mg (19.5%). Anal. Found: C, 26.70; H, 5.65; N, 5.10%. Calcd for  $\text{C}_{12}\text{H}_{30}\text{BCoF}_4\text{N}_2\text{P}_2\text{S}_4$ : C, 26.77; H, 5.62; N, 5.20%.

From the filtrate of red crystals of **c-0**, the  $\text{PF}_6^-$  salts of the isomers, *cis*-[Co(dtc)<sub>2</sub>(PMe<sub>3</sub>)<sub>2</sub>]PF<sub>6</sub> (**c-0'**: ca. 40%) and *trans*-[Co(dtc)<sub>2</sub>(PMe<sub>3</sub>)<sub>2</sub>]PF<sub>6</sub> (**t-0'**: ca. 60%), were precipitated by addition of a methanol solution (5 cm<sup>3</sup>) of  $\text{NH}_4\text{PF}_6$  (5 g). The precipitates were dissolved in a mixture of dichloromethane and methanol (1:2, 20 cm<sup>3</sup>) at 30 °C, and the filtered solution was cooled in a refrigerator overnight to give red prismatic crystals of pure **t-0'**. Yield: 272 mg (15.2%). Anal. Found: C, 24.16; H, 5.02; N, 4.75%. Calcd for  $\text{C}_{12}\text{H}_{30}\text{CoF}_6\text{N}_2\text{P}_3\text{S}_4$ : C, 24.16; H, 5.07; N, 4.70%. The filtrate was evaporated to 10 cm<sup>3</sup> in the open air to afford red prismatic crystals of **c-0'**, which were recrystallized from  $\text{CH}_2\text{Cl}_2/\text{CH}_3\text{OH}$  to give pure crystals of **c-0'**. Yield: 181 mg (10.1%). Anal. Found: C, 24.21; H, 4.89; N, 4.77%. Calcd for  $\text{C}_{12}\text{H}_{30}\text{CoF}_6\text{N}_2\text{P}_3\text{S}_4$ : C, 24.16; H, 5.07; N, 4.70%.

**Measurements.** The  $^1\text{H}$  and  $^{13}\text{C}$  NMR spectra were obtained at 30 °C on a JEOL GSX-400 spectrometer using tetramethylsilane as an internal reference. The  $^{31}\text{P}$  and  $^{59}\text{Co}$  NMR spectra were recorded at 30 °C on a JEOL Lambda 500 spectrometer using 85%  $\text{H}_3\text{PO}_4$  and [Co(dtc)<sub>3</sub>] (in  $\text{CDCl}_3$ ) as an external reference for  $^{31}\text{P}$  and  $^{59}\text{Co}$  NMR, respectively. The chemical shift of [Co(dtc)<sub>3</sub>] was set to be  $\delta$  6704.<sup>16</sup> UV-vis absorption spectra in  $\text{CH}_2\text{Cl}_2$  were measured on a Perkin-Elmer Lambda 19 spectrophotometer at room temperature.

**X-ray Crystallographic Study.** The X-ray diffraction data were measured at 23 °C on an automated Rigaku AFC-5R four-circle diffractometer equipped with a graphite-monochromated Mo  $K\alpha$  radiation ( $\lambda = 0.71073$  Å). For **t-3**·H<sub>2</sub>O, the intensities collected up to  $2\theta = 55^\circ$  by the  $\omega$  scan mode were corrected for Lorentz-polarization factors and for absorption effects by the numerical integration method.<sup>17</sup> For the others, the  $2\theta$ - $\omega$  scan method was applied to obtain the data up to  $2\theta = 60^\circ$ , and the absorption corrections were made by an empirical method using three sets of  $\psi$ -scan data.<sup>18</sup> The structures were solved by the direct method using SHELXS86 program,<sup>19</sup> and refined on  $F^2$  (with all independent reflections) by means of SHELXL97 program.<sup>20</sup> All calculations were carried out using a TeXsan software package.<sup>21</sup> Crystal data are collected in Table 1; the details for each analysis are given below.

Compounds **t-0** and **t-1** were found to crystallize in a triclinic space group  $P\bar{1}$  with  $Z = 1$  and in a monoclinic space group  $P2_1/n$  with  $Z = 2$ , respectively. In each crystal the Co atom was located on a crystallographic center of symmetry. The B atom of  $\text{BF}_4^-$  anion was also located on a center of symmetry, and the F atoms showed severe positional disorder. The apparent structure of the counter anion was an octahedral  $\text{B}(\frac{2}{3}\text{F})_6^-$  with the F atoms having a large thermal ellipsoid, although the existence of  $\text{BF}_4^-$  in the crystals was confirmed by their infrared spectra and elemental analyses.

For compound **t-2**, the Laue group (4/*mmm*) and the systematic absences ( $h + k + l = \text{odd}$ ,  $2h + l = 4n$ ) indicated that the space

group was either  $\bar{I}4_2d$  or  $I4_1md$ . The structure was solved reasonably on the assumption of  $\bar{I}4_2d$ , but not on that of  $I4_1md$ . Both Co and B atoms were located on a crystallographic two-fold axis. Two of the F atoms of  $\text{BF}_4^-$  anion showed positional disorder that was related to the crystallographic two-fold symmetry.

Compound **t-3**·H<sub>2</sub>O was found to crystallize in a monoclinic space group  $P2_1$  with  $Z = 4$ , indicating that two crystallographically independent complex cations, two  $\text{BF}_4^-$  anions and two solvated water molecules exist in an asymmetric unit. Assumption of the corresponding centrosymmetric space group  $P2_1/m$  did not give any reasonable structure solution.

Since the crystal of **c-0** decomposed gradually during the data collection, a linear decay correction was applied, although no solvent molecules of crystallization were found in the structure analysis. The space group was assumed to be a centrosymmetric  $C2/c$ , which gave a reasonable structure solution with  $Z = 4$ . The Co atom located on a crystallographic  $C_2$  axis. The counter anion was located close to a crystallographic center of symmetry, so that the B and two F atoms were treated as positionally disordered ones.

The structure of compound **c-1'** could be solved without any difficulty on the assumption of centrosymmetric space group  $P\bar{1}$  with  $Z = 2$ .

Tables of crystallographic data (excluding structure factors), atomic coordinates, thermal parameters, full lists of bond lengths and angles, and some additional figures showing the molecular structures of the complexes are deposited as Document No. 74063 at the Office of the Editor of Bull. Chem. Soc. Jpn. Crystallographic data have been deposited at the CCDC, 12 Union Road, Cambridge CB2 1EZ, UK and copies can be obtained on request, free of charge, by quoting the publication citation and deposition numbers CCDC 169101–169106.

## Results and Discussion

**Preparation and Structural Characterization of Complexes.** In previous papers, we have described the synthesis of mixed-ligand cobalt(III) complexes containing dtc and phosphines<sup>9</sup> or phosphites<sup>10</sup> by oxidation of an ethanolic mixture of  $\text{Co}(\text{BF}_4)_2 \cdot 6\text{H}_2\text{O}$  and either phosphine or phosphite with tetramethylthiuram disulfide. While such a reaction with phosphite ( $\text{P}(\text{OMe})_3$ ,  $\text{P}(\text{OEt})_3$ , or  $\text{P}(\text{OCH}_2)_3\text{CEt}$ ) gave *cis*-[Co(dtc)<sub>2</sub>(phosphite)<sub>2</sub>]<sup>+</sup> and [Co(dtc)(phosphite)<sub>4</sub>]<sup>2+</sup>, a similar reaction with  $\text{PPh}_3$  afforded only *trans*-[Co(dtc)<sub>2</sub>( $\text{PPh}_3$ )<sub>2</sub>]BF<sub>4</sub> (**t-3**); neither the *cis*-isomer nor the tetrakis( $\text{PPh}_3$ ) complexes were obtained from the reaction mixture.<sup>9</sup> When the reaction was performed in a molar ratio of  $\text{Co}^{2+}:\text{PPh}_3:\text{disulfide} = 1:2:1$ , the isolated yield of complex **t-3** was improved to 45%.

A similar reaction of  $\text{Co}(\text{BF}_4)_2 \cdot 6\text{H}_2\text{O}$ ,  $\text{PMePh}_2$  and the disulfide in a mixture of methanol and dichloromethane yielded *trans*-[Co(dtc)<sub>2</sub>( $\text{PMePh}_2$ )<sub>2</sub>]BF<sub>4</sub> (**t-2**) as a main product (60% isolated yield). The geometrical structure of the product was determined by the  $^1\text{H}$  and  $^{13}\text{C}$  NMR spectra, both of which showed a singlet resonance for N-CH<sub>3</sub> (Table 2), and this structure was confirmed by X-ray analysis (vide infra). The corresponding *cis*-isomer, *cis*-[Co(dtc)<sub>2</sub>( $\text{PMePh}_2$ )<sub>2</sub>]BF<sub>4</sub>, could not be isolated, but the existence (ca. 5%) in the crude reaction product was detected by  $^1\text{H}$  NMR spectroscopy: a filled-in doublet resonance at  $\delta$  1.850 for P-CH<sub>3</sub> and two singlet ones at  $\delta$  2.789 and 2.985 for N-CH<sub>3</sub>.

In the case of  $\text{PMe}_2\text{Ph}$ , both *trans*- and *cis*-isomers could be isolated from the reaction mixture. After the chromatographic

Table 1. Crystallographic Data

Compounds	<i>t</i> -0	<i>t</i> -1	<i>t</i> -2	<i>t</i> -3·H <sub>2</sub> O	<i>c</i> -0	<i>c</i> -1'
Chemical formula	C <sub>12</sub> H <sub>30</sub> BCoF <sub>4</sub> N <sub>2</sub> P <sub>2</sub> S <sub>4</sub>	C <sub>22</sub> H <sub>34</sub> BCoF <sub>4</sub> N <sub>2</sub> P <sub>2</sub> S <sub>4</sub>	C <sub>32</sub> H <sub>38</sub> BCoF <sub>4</sub> N <sub>2</sub> P <sub>2</sub> S <sub>4</sub>	C <sub>42</sub> H <sub>44</sub> BCoF <sub>4</sub> N <sub>2</sub> OP <sub>2</sub> S <sub>4</sub>	C <sub>12</sub> H <sub>30</sub> BCoF <sub>4</sub> N <sub>2</sub> P <sub>2</sub> S <sub>4</sub>	C <sub>22</sub> H <sub>34</sub> CoF <sub>6</sub> N <sub>2</sub> P <sub>3</sub> S <sub>4</sub>
Formula weight	538.30	662.43	786.56	928.71	538.30	720.59
Color and shape of crystal	red brown, column	red, prism	dark red, prism	purple, plate	red, prism	red, plate
Size of specimen (mm)	0.50×0.30×0.20	0.60×0.40×0.30	0.20×0.20×0.20	0.35×0.28×0.26	0.20×0.20×0.14	0.40×0.35×0.20
Crystal system	triclinic	monoclinic	tetragonal	monoclinic	monoclinic	triclinic
Space group	$P\bar{1}$	$P2_1/n$	$I\bar{4}2d$	$P2_1$	$C2/c$	$P\bar{1}$
<i>a</i> / Å	8.667(4)	6.630(3)	21.622(3)	9.970(5)	20.883(5)	14.481(2)
<i>b</i> / Å	11.170(3)	15.689(3)	21.622	32.176(5)	11.681(6)	14.715(2)
<i>c</i> / Å	6.425(1)	14.447(3)	15.620(5)	14.230(3)	12.351(10)	7.433(1)
$\alpha$ / °	90.86(2)	90	90	90	90	94.78(1)
$\beta$ / °	100.66(3)	92.23(3)	90	91.18(2)	123.01(3)	94.26(1)
$\gamma$ / °	78.43(3)	90	90	90	90	92.40(1)
<i>U</i> / Å <sup>3</sup>	598.7(3)	1501.6(7)	7303(3)	4564(2)	2526(2)	1572.3(3)
<i>Z</i>	1	2	8	4	4	2
<i>D</i> <sub>calc</sub> / Mg m <sup>-3</sup>	1.493	1.465	1.431	1.352	1.415	1.522
<i>F</i> (000)	278	684	3248	1920	1112	740
$\mu$ (Mo <i>K</i> α) / mm <sup>-1</sup>	1.230	0.997	0.833	0.679	1.166	1.016
Transmission factors	0.732–1.000	0.893–1.000	0.946–1.000	0.818–0.853	0.766–1.000	0.857–1.000
<i>R</i> <sub>int</sub>	0.013	0.018	0.053	0.035	0.166	0.014
No. of independent reflections	3480	4371	2888	10696	3738	9189
No. of parameters	135	179	222	1034	137	351
<i>R</i> 1 ( <i>F</i> <sup>2</sup> : <i>F</i> <sub>o</sub> <sup>2</sup> > 2σ( <i>F</i> <sub>o</sub> <sup>2</sup> ))	0.045	0.037	0.044	0.074	0.062	0.036
<i>wR</i> 2 ( <i>F</i> <sup>2</sup> : all data)	0.136	0.119	0.107	0.218	0.186	0.109
GOF	1.027	1.010	1.008	1.019	1.046	1.031

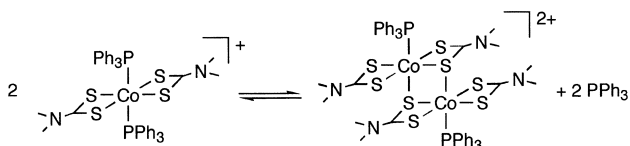
Table 2. Selected NMR Data<sup>a)</sup> in δ from TMS for <sup>1</sup>H and <sup>13</sup>C; 85% H<sub>3</sub>PO<sub>4</sub> for <sup>31</sup>P; K<sub>3</sub>[Co(CN)<sub>6</sub>] for <sup>59</sup>Co

Complex	<sup>1</sup> H		<sup>13</sup> C		<sup>31</sup> P	<sup>59</sup> Co	
	P-CH <sub>3</sub>	N-CH <sub>3</sub>	P-CH <sub>3</sub>	N-CH <sub>3</sub>			
<i>t</i> -0	1.477 (vt)	3.296 (t)	12.93 (vt)	39.07	202.91	-2.77	3560
<i>t</i> -1	1.823 (vt)	2.874 (t)	12.68 (vt)	38.56	201.85	4.79	3575
<i>t</i> -2	2.104 (vt)	2.659	11.50 (vt)	38.29	199.32	14.21	3713
<i>t</i> -3	—	2.387	—	37.70	198.00	25.17	—
<i>c</i> -0	1.524 (fd)	3.243	15.16 (vt)	38.06	201.49	7.27	3144
		3.304		38.37			
<i>c</i> -1'	1.482 (fd)	3.256	9.69 (vt)	38.10	201.24	7.45	3368
	1.574 (fd)	3.297	16.21 (vt)	38.54	—	—	—
[Co(dtc) <sub>3</sub> ]	—	3.253	—	37.67	204.90	—	6704

a) at 30°C in CDCl<sub>3</sub>, except for <sup>59</sup>Co NMR of *t*-0, *t*-1, and *t*-2 which are in CD<sub>3</sub>CN. The symbols in parenthesis, fd, vt and t denote filled-in doublet, virtual triplet and triplet, respectively, and the other signals are singlet.

separation from by-products, the obtained product was a mixture of *trans*-[Co(dtc)<sub>2</sub>(PMe<sub>2</sub>Ph)<sub>2</sub>]BF<sub>4</sub> (*t*-1: 42%) and *cis*-[Co(dtc)<sub>2</sub>(PMe<sub>2</sub>Ph)<sub>2</sub>]BF<sub>4</sub> (*c*-1: 58%), which was determined by the <sup>1</sup>H NMR spectrum. The isomers were separated from each other by fractional recrystallization of the BF<sub>4</sub><sup>-</sup> or PF<sub>6</sub><sup>-</sup> salt (see Experimental). The <sup>1</sup>H and <sup>13</sup>C NMR spectra of *t*-1 are

similar to those of *t*-2, except for the observation of a weak coupling between N-CH<sub>3</sub> and P nuclei to give a triplet resonance for N-CH<sub>3</sub>. The <sup>1</sup>H and <sup>13</sup>C NMR spectra of *c*-1' give two filled-in doublet and two virtual triplet signals, respectively, for P-CH<sub>3</sub> groups, which is consistent to the C<sub>2</sub> symmetry of the cationic complex.



Scheme 1. A plausible equilibrium in an acetonitrile solution of complex **t-3**.

For  $\text{PMe}_3$  complexes, the product obtained by a similar method to the above  $\text{PMe}_2\text{Ph}$  complexes was found to be a mixture of *trans*- $[\text{Co}(\text{dtc})_2(\text{PMe}_3)_2]\text{BF}_4$  (**t-0**: 35%) and *cis*- $[\text{Co}(\text{dtc})_2(\text{PMe}_3)_2]\text{BF}_4$  (**c-0**: 65%). The formation of the *trans*-isomer is in contrast to the preparation of  $[\text{Co}(\text{acac})_2(\text{PMe}_3)_2]^+$  by oxidation of an ethanolic mixture of  $[\text{Co}(\text{acac})_2(\text{H}_2\text{O})_2]$  and  $\text{PMe}_3$  by  $\text{PbO}_2/\text{AcOH}$ , which gave only the *cis*-isomer.<sup>4</sup> The isomers were separated by fractional recrystallization of the  $\text{BF}_4^-$  or  $\text{PF}_6^-$  salt (see Experimental), and the isolated yields of the complexes are: **c-0**, 20%; *cis*- $[\text{Co}(\text{dtc})_2(\text{PMe}_3)_2]\text{PF}_6$  (**c-0'**), 10%; and *trans*- $[\text{Co}(\text{dtc})_2(\text{PMe}_3)_2]\text{PF}_6$  (**t-0'**), 15%. We have also attempted to prepare **t-0** by a reaction of **t-3** with  $\text{PMe}_3$ , analogously to the preparative method of *trans*- $[\text{Co}(\text{acac})_2(\text{PMe}_3)_2]\text{PF}_6$  from *trans*- $[\text{Co}(\text{acac})_2(\text{PPh}_3)_2]\text{PF}_6$ .<sup>2</sup> This method was successful, and complex **t-0** could be obtained in 94% isolated yield without any formation of **c-0** and the other impurities. This indicates that complex **t-3** may be a good starting material for the complexes having a *trans*- $[\text{Co}(\text{dtc})_2(\text{ligand})_2]^+$  moiety.

$^1\text{H}$ ,  $^{13}\text{C}$ , and  $^{31}\text{P}$  NMR spectroscopy suggest that, although the  $\text{PPh}_3$  complex of **t-3** is stable in dichloromethane and chloroform, in acetonitrile, it dissociates one of the  $\text{PPh}_3$  ligands and exists as an equilibrium mixture together with the dissociated product, which can probably be assigned as *trans*( $P, \mu(S)$ )- $[\{\text{Co}(\text{dtc}-\kappa^2S)(\text{PPh}_3)_2(\mu(S)-\text{dtc}-\kappa^2S, S')\}_2]^{2+}$  (Scheme 1) by analogy of the  $^1\text{H}$  NMR spectrum to that of the corresponding  $\text{P}(\text{OMe})_2\text{Ph}$  complex.<sup>13</sup> All of the other isolated bis(dtc) complexes are fairly stable in dichloromethane, chloroform, acetonitrile, and methanol, even when the solvents are wet. The stability of *trans*- $[\text{Co}(\text{dtc})_2(\text{PMe}_3, \text{PMe}_2\text{Ph} \text{ or } \text{PMe-Ph}_2)_2]\text{BF}_4$  toward hydrolysis is in contrast to the analogous bis(acac) complexes, *trans*- $[\text{Co}(\text{acac})_2(\text{PMe}_{3-n}\text{Ph}_n)_2]\text{PF}_6$ , which are easily hydrolyzed in wet organic solvents.<sup>2,4</sup>

**Crystal Structures. The *cis*-Isomers: Electronic *trans* Influences of  $\text{PMe}_3$  and  $\text{PMe}_2\text{Ph}$ .** The X-ray crystallographic analyses for **c-0** and **c-1'** confirmed that the complexes have *cis* configuration for the phosphine ligands. The molecular structures of the cationic complexes in **c-0** and **c-1'** are shown in Fig. 1, and selected bond lengths and angles are listed in Table 3. In the  $\text{PMe}_3$  complex the Co atom is sited on a crystallographic  $C_2$  axis, which bisects the  $\text{P}(1)\text{--Co--P}(1')$  and  $\text{S}(2)\text{--Co--S}(2')$  angles. Both complexes have a similar structure with respect to the  $\text{Co}(\text{dtc})_2$  moiety to those in *cis*- $[\text{Co}(\text{dtc})_2\{\text{P}(\text{OCH}_2)_3\text{CEt}\}_2]\text{BF}_4$ ,<sup>10</sup>  $[\text{Co}(\text{dtc})_2(\text{dmpf})]\text{BF}_4$  ( $\text{dmpf} = 1,1'$ -bis(dimethylphosphino)ferrocene)<sup>8</sup> and  $[\text{Co}(\text{dtc})_3]$ ,<sup>15</sup> except for a slight deviation of the Co–S bond lengths described below. The bite angles of dtc are  $75.07(7)^\circ$  and average  $76.15(2)^\circ$  for **c-0** and **c-1'**, respectively, which are a little smaller than the angles in  $[\text{Co}(\text{dtc})_3]$  (average  $76.4^\circ$ ).

The Co–S bond lengths in *cis*- $[\text{Co}(\text{dtc})_2(\text{P-ligand})_2]^+$  provide a good measure to elucidate the strength of electronic

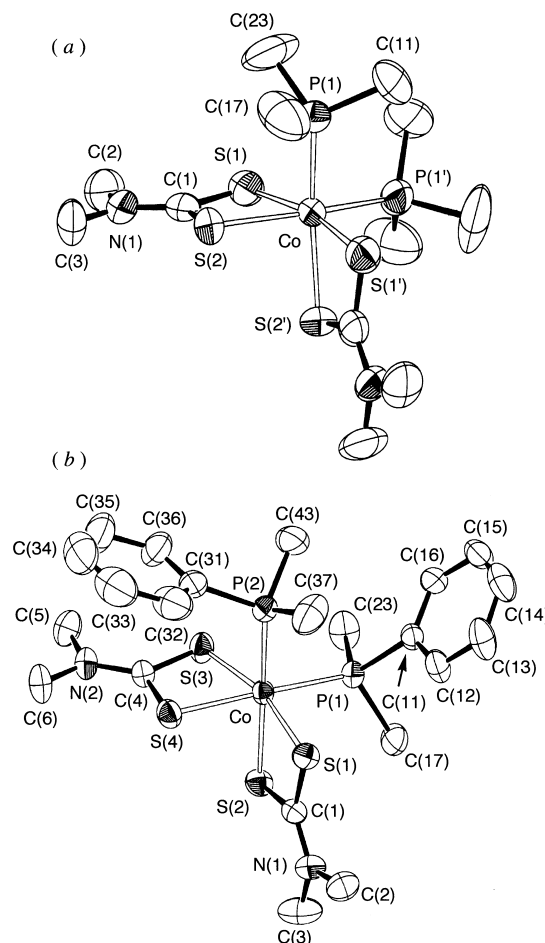


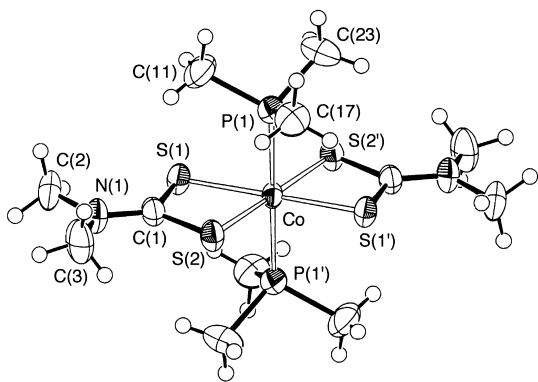
Fig. 1. Perspective drawings of the cationic complexes in (a) *cis*- $[\text{Co}(\text{dtc})_2(\text{PMe}_3)_2]\text{BF}_4$  (**c-0**: 40% probability level) and (b) *cis*- $[\text{Co}(\text{dtc})_2(\text{PMe}_2\text{Ph})_2]\text{PF}_6$  (**c-1'**: 50% probability level). For both figures hydrogen atoms are omitted for clarity.

*trans* influences of the P-ligands, unless there exists a stacking interaction between the dtc plane and the phenyl ring of P-ligand (vide infra). In the  $\text{PMe}_3$  complex (**c-0**), the Co–S(2) bond is longer by  $0.055 \text{ \AA}$  than the Co–S(1) bond (see Table 3), owing to the electronic *trans* influence of  $\text{PMe}_3$ . For the  $\text{PMe}_2\text{Ph}$  complex (**c-1'**), there is an intramolecular  $\pi$ – $\pi$  stacking interaction between one of the dtc ligands and the phenyl ring of C(31)–C(36), but the other dtc has no such interaction, as seen from Fig. 1b. Therefore, we will compare only the Co–S(1) and Co–S(2) bond lengths for evaluating the electronic *trans* influence of  $\text{PMe}_2\text{Ph}$ . The Co–S(2) bond *trans* to  $\text{P}(\text{PMe}_2\text{Ph})$  is longer by  $0.032 \text{ \AA}$  than the Co–S(1) bond *trans* to S(dtc). In the  $\text{P}(\text{OCH}_2)_3\text{CEt}$  complex, *cis*- $[\text{Co}(\text{dtc})_2\{\text{P}(\text{OCH}_2)_3\text{CEt}\}_2]\text{BF}_4$ , the difference between two kinds of Co–S bond lengths is only  $0.016 \text{ \AA}$ .<sup>10</sup> Thus, the order of the strengths of electronic *trans* influence in *cis*- $[\text{Co}(\text{dtc})_2(\text{P-ligand})_2]^+$  is suggested to be  $\text{PMe}_3 > \text{PMe}_2\text{Ph} > \text{P}(\text{OCH}_2)_3\text{CEt}$ . This order coincides with the strength of the  $\sigma$ -donicity of the P-ligands:  $\text{PMe}_3$  ( $\chi_d = 8.55$ )  $>$   $\text{PMe}_2\text{Ph}$  (10.60)  $>$   $\text{P}(\text{OCH}_2)_3\text{CEt}$  (18.39).<sup>22</sup>

Two Co–P bond lengths in the  $\text{PMe}_2\text{Ph}$  complex (**c-1'**) are  $2.2795(6)$  and  $2.2637(7) \text{ \AA}$ , showing a relatively large discrep-

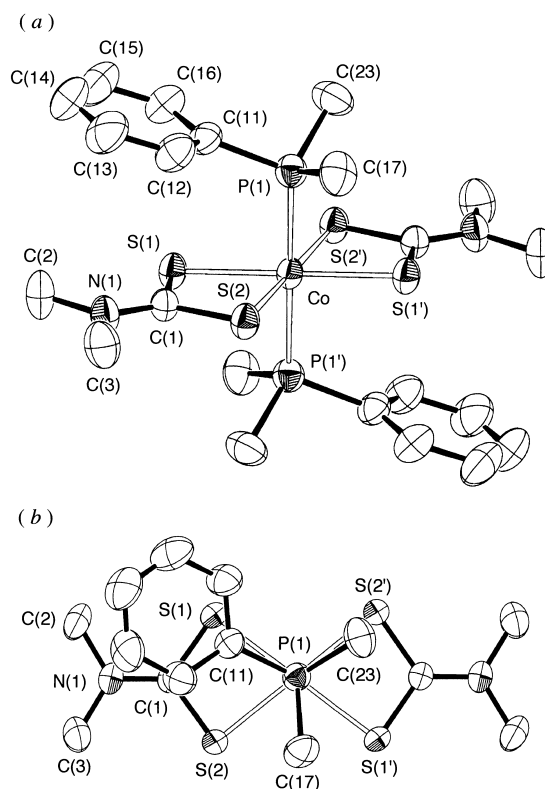
Table 3. Selected Bond Lengths (Å) and Angles (°) of *cis*-[Co(dtc)<sub>2</sub>(PMe<sub>3</sub>)<sub>2</sub>]BF<sub>4</sub> and *cis*-[Co(dtc)<sub>2</sub>(PMe<sub>2</sub>Ph)<sub>2</sub>]PF<sub>6</sub>

<i>cis</i> -[Co(dtc) <sub>2</sub> (PMe <sub>3</sub> ) <sub>2</sub> ]BF <sub>4</sub> ( <b>c-0</b> )					
Co–P(1)	2.200(2)	Co–S(1)	2.255(2)	Co–S(2)	2.310(2)
S(1)–Co–S(2)	75.07(7)	P(1)–Co–P(1')	96.8(1)		
P(1)–Co–S(2')	164.60(7)	S(1)–Co–S(1')	167.4(1)		
<i>cis</i> -[Co(dtc) <sub>2</sub> (PMe <sub>2</sub> Ph) <sub>2</sub> ]PF <sub>6</sub> ( <b>c-1'</b> )					
Co–P(1)	2.2795(6)	Co–S(1)	2.2578(7)	Co–S(2)	2.2902(7)
Co–P(2)	2.2637(7)	Co–S(3)	2.2791(7)	Co–S(4)	2.2921(7)
S(1)–Co–S(2)	76.31(2)	S(3)–Co–S(4)	75.99(2)		
P(1)–Co–P(2)	95.14(2)	S(1)–Co–S(3)	164.80(2)		
P(1)–Co–S(4)	173.03(2)	P(2)–Co–S(2)	173.46(3)		

Fig. 2. Perspective drawing (50% probability level) of the cationic complex in *trans*-[Co(dtc)<sub>2</sub>(PMe<sub>3</sub>)<sub>2</sub>]BF<sub>4</sub> (**t-0**).

ancy (0.016 Å) between them. Such a difference in the Co–P(PMe<sub>2</sub>Ph) bond lengths may be caused by the above-mentioned stacking interaction between dtc and PMe<sub>2</sub>Ph, which makes the interacting Co–S(dtc) bond shorter, as clarified in the next section. In fact, the Co–P(2) bond of the interacting PMe<sub>2</sub>Ph is shorter than the Co–P(1) bond of the non-interacting one. However, we can not claim any generality of such a relationship between the Co–P bond lengths and the stacking interaction at present, because there are no other examples relevant to the relationship.

The Co–P bond length in the PMe<sub>3</sub> complex (**c-0**) is 2.220(2) Å, which is shorter than those in the PMe<sub>2</sub>Ph complex (**c-1'**). The corresponding Co–P bond lengths in *cis*-[Co(dtc)<sub>2</sub>{P(OCH<sub>2</sub>)<sub>3</sub>CEt}<sub>2</sub>]BF<sub>4</sub>, 2.169(1) and 2.172(1) Å,<sup>10</sup> are even shorter, in accordance with the cone angles of P-ligands: PMe<sub>3</sub>, 118°; PMe<sub>2</sub>Ph, 122°; P(OCH<sub>2</sub>)<sub>3</sub>CEt, 101°.<sup>23</sup> However, for PHPh<sub>2</sub> having a larger cone angle (126°), the corresponding Co–P bond lengths in *cis*-[Co(dtc)<sub>2</sub>(PHPh<sub>2</sub>)<sub>2</sub>]BF<sub>4</sub>·CH<sub>3</sub>CN·0.5Et<sub>2</sub>O are unexpectedly short, 2.2340(6) and 2.2258(7) Å.<sup>14</sup> Moreover, the P–Co–P bond angles in the PMe<sub>3</sub>, PMe<sub>2</sub>Ph, P(OCH<sub>2</sub>)<sub>3</sub>CEt and PHPh<sub>2</sub> complexes are 96.8(2), 95.14(2), 92.55(5) and 90.51(2)°, respectively. These observations suggest that, although the cone angles of P-ligands would be important as well, the other steric effects such as mutual orientation of their substituent groups (including the above-mentioned intramolecular stacking interaction with a dtc moiety) and the electronic (σ-donor/π-acceptor) character of P-ligands must be taken into consideration to specify the Co–P bond

Fig. 3. (a) Perspective and (b) top views (50% probability level; hydrogen atoms are omitted) of the cationic complex in *trans*-[Co(dtc)<sub>2</sub>(PMe<sub>2</sub>Ph)<sub>2</sub>]BF<sub>4</sub> (**t-1**). For the figure of (b) the PMe<sub>2</sub>Ph ligand below the equatorial CoS<sub>4</sub> plane is omitted for clarity.

lengths and P–Co–P angles in *cis*-[Co(dtc)<sub>2</sub>(P-ligand)<sub>2</sub>]<sup>+</sup>-type complexes.

#### The *trans*-Isomers: Steric *trans* Influence via the Equatorial dtc Ligands for the Elongation of Co–P Bond.

Perspective drawings of the complex cations in *trans*-[Co(dtc)<sub>2</sub>(PMe<sub>3</sub>)<sub>2</sub>]BF<sub>4</sub> (**t-0**) and *trans*-[Co(dtc)<sub>2</sub>(PMe<sub>2</sub>Ph)<sub>2</sub>]BF<sub>4</sub> (**t-1**) are shown in Figs. 2 and 3, respectively, and selected bond lengths and angles are listed in Table 4. In both complexes the Co atom is located at a crystallographic inversion center, and the complex cation has *C<sub>i</sub>* molecular symmetry. The Co–S bond lengths in **t-0** (average 2.270 Å) are comparable to those in [Co(dtc)<sub>3</sub>] (average 2.264 Å).<sup>15</sup> Although the average Co–S

Table 4. Selected Bond Lengths (Å) and Angles (°) of *trans*-[Co(dtc)<sub>2</sub>(PMe<sub>3-n</sub>Ph<sub>n</sub>)<sub>2</sub>]BF<sub>4</sub>·(H<sub>2</sub>O)

<i>trans</i> -[Co(dtc) <sub>2</sub> (PMe <sub>3</sub> ) <sub>2</sub> ]BF <sub>4</sub> ( <b>t-0</b> )					
Co–P(1)	2.287(1)	Co–S(1)	2.2681(9)	Co–S(2)	2.2715(8)
S(1)–Co–S(2)	76.86(3)				
<i>trans</i> -[Co(dtc) <sub>2</sub> (PMe <sub>2</sub> Ph) <sub>2</sub> ]BF <sub>4</sub> ( <b>t-1</b> )					
Co–P(1)	2.2843(8)	Co–S(1)	2.2626(7)	Co–S(2)	2.2782(9)
S(1)–Co–S(2)	76.75(3)				
<i>trans</i> -[Co(dtc) <sub>2</sub> (PMePh <sub>2</sub> ) <sub>2</sub> ]BF <sub>4</sub> ( <b>t-2</b> )					
Co–P(1)	2.303(1)	Co–S(1)	2.264(1)	Co–S(2)	2.293(1)
S(1)–Co–S(2)	76.18(4)		P(1)–Co–P(1')	169.66(7)	
S(1)–Co–S(1')	94.38(6)		S(2)–Co–S(2')	113.29(6)	
<i>trans</i> -[Co(dtc) <sub>2</sub> (PPh <sub>3</sub> ) <sub>2</sub> ]BF <sub>4</sub> ·H <sub>2</sub> O ( <b>t-3</b> ·H <sub>2</sub> O)					
Co(1)–P(1)	2.319(3)	Co(1)–S(1)	2.242(3)	Co(1)–S(2)	2.285(3)
Co(1)–P(2)	2.303(3)	Co(1)–S(3)	2.251(3)	Co(1)–S(4)	2.283(3)
Co(51)–P(51)	2.331(4)	Co(51)–S(51)	2.254(4)	Co(51)–S(52)	2.271(3)
Co(51)–P(52)	2.311(3)	Co(51)–S(53)	2.245(3)	Co(51)–S(54)	2.279(3)
S(1)–Co(1)–S(2)	76.2(1)	S(3)–Co(1)–S(4)	76.6(1)		
S(1)–Co(1)–S(3)	94.0(1)	S(2)–Co(1)–S(4)	113.4(1)		
S(51)–Co(51)–S(52)	76.0(1)	S(53)–Co(51)–S(54)	76.1(1)		
S(51)–Co(51)–S(53)	94.3(1)	S(52)–Co(51)–S(54)	113.6(1)		
P(1)–Co(1)–P(2)	168.3(1)	P(51)–Co(51)–P(52)	167.1(1)		

bond length in **t-1** (2.270 Å) is just the same as that in **t-0**, there is a rather large discrepancy between two Co–S bond lengths in **t-1** (Co–S(1) = 2.2626(7) and Co–S(2) = 2.2782(9) Å). This discrepancy would be related to the intramolecular  $\pi$ – $\pi$  stacking interaction between the dtc moiety and the phenyl substituent of PMe<sub>2</sub>Ph. As seen from Fig. 3b, the phenyl ring is located just above the S(1) atom, and the dihedral angle between the dtc mean plane and the phenyl ring is 18.0(1)°. Such a stacking interaction between dtc plane and phenyl ring, accompanied with a shortening of the interacting Co–S bond lengths, is also observed in the analogous PMePh<sub>2</sub> (**t-2**) and PPh<sub>3</sub> (**t-3**) complexes (vide infra and Table 4). Thus, it should be noted that the intramolecular  $\pi$ – $\pi$  stacking makes the interacting Co–S bond shorter.

The Co–P bond length in the PMe<sub>3</sub> complex (**t-0**: 2.287(1) Å) is comparable to (or slightly longer than) that in the PMe<sub>2</sub>Ph one (**t-1**: 2.2843(8) Å), in contrast to those of the *cis*-complexes. The differences in Co–P bond lengths between the *trans*- and *cis*-isomers are 0.087 Å for the PMe<sub>3</sub> complexes and 0.021 Å<sup>24</sup> for the PMe<sub>2</sub>Ph ones. This is also due to the fact that the electronic *trans* influence of PMe<sub>3</sub> is stronger than that of PMe<sub>2</sub>Ph, which elongates the mutually *trans* Co–P bonds. Since there would be no difference in the electronic *cis* influence,<sup>25</sup> a smaller steric requirement of PMe<sub>3</sub> would make the Co–P(PMe<sub>3</sub>) bonds shorter than the Co–P(PMe<sub>2</sub>Ph) bonds, while a stronger  $\sigma$ -donicity of PMe<sub>3</sub> induces the stronger electronic *trans* influence, leading to mutual elongation of the Co–P(PMe<sub>3</sub>) bonds. Therefore, the comparable Co–P bond lengths observed in **t-0** and **t-1** result from the competition of these opposite effects. We have previously found a similar result for the Co–P bonds in the analogous acac complexes: *trans*-[Co(acac)<sub>2</sub>(PMe<sub>3</sub> or PMe<sub>2</sub>Ph)<sub>2</sub>]<sup>+</sup>.<sup>1</sup>

The molecular structure of *trans*-[Co(dtc)<sub>2</sub>(PMePh<sub>2</sub>)<sub>2</sub>]<sup>+</sup> in **t-2** is shown in Fig. 4a. The complex cation has molecular C<sub>2</sub>

symmetry; the Co atom is sited on a crystallographic C<sub>2</sub> axis, which bisects the S(1)–Co–S(1') and P(1)–Co–P(1') angles. One of the phenyl rings, C(11)–C(16), of PMePh<sub>2</sub> is located above the S(1) atom, similar to the PMe<sub>2</sub>Ph complex **t-1**, with the dihedral angle of 5.24(6)° between the dtc mean plane and the phenyl ring. The Co–S(1) bond is shorter by 0.029 Å than the Co–S(2) bond. The other phenyl ring, C(17)–C(22), is located in the cleft between S(2) and S(2') atoms, and oriented perpendicularly to the equatorial CoS<sub>4</sub> plane, the angle between the phenyl ring and the CoS<sub>4</sub> mean plane being 87.1(1)°. This is also the case in another side of the equatorial CoS<sub>4</sub> plane, as suggested from molecular C<sub>2</sub> symmetry (Fig. 4b). Such a conformation of the phenyl rings is remarkably different from that in *trans*-[Co(acac)<sub>2</sub>(PMePh<sub>2</sub>)<sub>2</sub>]PF<sub>6</sub>.<sup>3</sup> Since dtc is a sterically more compact didentate ligand than acac, as indicated by the smaller bite angle, the cleft in the equatorial Co(dtc)<sub>2</sub> coordination plane is much larger than that of the Co(acac)<sub>2</sub> plane, as illustrated in Fig. 5. Moreover, since the coordination of dtc is rather flexible as far as the deviation from the regular octahedron of the Co<sup>III</sup> coordination sphere, the cleft of the S(2)–Co–S(2') side (113.29(6)°) is larger than the other S(1)–Co–S(1') side (94.38(6)°). As indicated in Fig. 4b by the space filling model, the *o*-hydrogen atom of each phenyl ring oriented perpendicularly is just fitted into the larger cleft between S(2) and S(2') atoms.

Similar structural characteristics to the above PMePh<sub>2</sub> complex are also found in the PPh<sub>3</sub> complex, *trans*-[Co(dtc)<sub>2</sub>(PPh<sub>3</sub>)<sub>2</sub>]BF<sub>4</sub> (**t-3**). There are two crystallographically independent complex cations: cation A with Co(1) atom and cation B with Co(51). A perspective view of the cation A is depicted in Fig. 6, and the molecular structure of cation B is very similar to that of A. Both complex cations have, not a crystallographically imposed, but a pseudo molecular C<sub>2</sub> symmetry. One of three phenyl rings of PPh<sub>3</sub> is perpendicularly

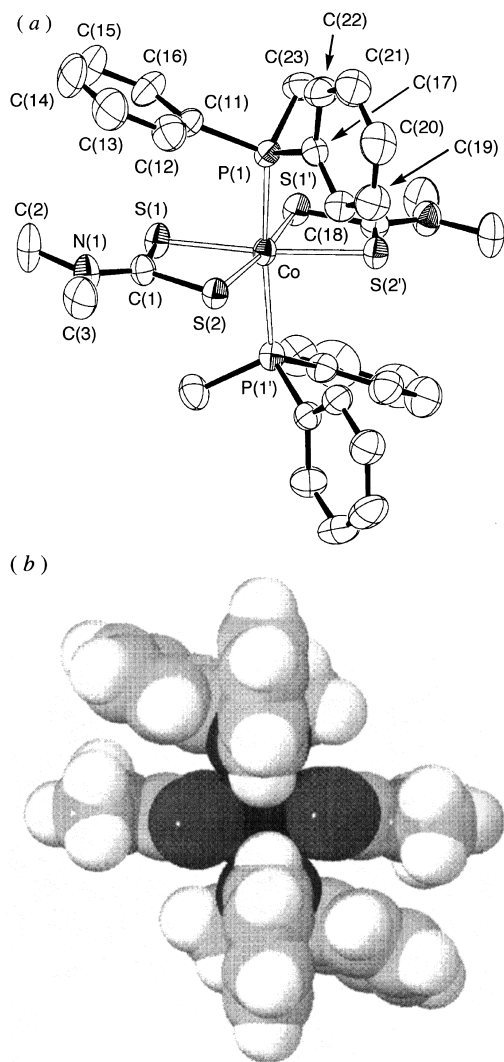


Fig. 4. (a) Perspective drawing (50% probability level; hydrogen atoms are omitted) of the cationic complex in  $\text{trans-}[\text{Co}(\text{dtc})_2(\text{PMePh}_2)_2]\text{BF}_4$  (**t-2**). (b) Space filling model of the cationic complex viewed from the bisector of the  $\text{S}(2)\text{-Co-S}(2')$  angle.

oriented to the larger cleft in the equatorial  $\text{Co}(\text{dtc})_2$  plane; the dihedral angles between the phenyl ring and the  $\text{CoS}_4$  mean plane are  $83.8(6)\text{-}89.6(3)^\circ$ ; the angles of  $\text{S}(1)\text{-Co}(1)\text{-S}(3)$  and  $\text{S}(51)\text{-Co}(51)\text{-S}(53)$  average  $94.2^\circ$ , while those of  $\text{S}(2)\text{-Co}(1)\text{-S}(4)$  and  $\text{S}(52)\text{-Co}(51)\text{-S}(54)$  average  $113.5^\circ$ .

The compactness and flexibility of dtc coordination result in reduction of the steric interaction from the equatorial ligands to elongate the axial  $\text{Co-P}$  bonds in  $\text{trans-}[\text{Co}(\text{dtc})_2(\text{PMe}_{3-n}\text{Ph}_n)_2]\text{BF}_4$ , when compared to those in  $\text{trans-}[\text{Co}(\text{acac})_2(\text{PMe}_{3-n}\text{Ph}_n)_2]\text{PF}_6$ . In Fig. 7, the  $\text{Co-P}$  bond lengths in the above two series of complexes, together with those in the related complexes, are plotted against the crystallographic cone angle<sup>26</sup> of  $\text{PMe}_{3-n}\text{Ph}_n$ . The  $\text{Co-P}$  bond lengths in **t-0**, **t-1** and **t-2** are shorter by 0.020, 0.017 and 0.026 Å, respectively, than those of the corresponding acac complexes; this fact is indicative of reduction of the steric interaction from the equatorial ligands. The shortening of the  $\text{Co-P}$  bond lengths is quite remarkable for the  $\text{PPh}_3$  complexes. The average  $\text{Co-P}$  bond

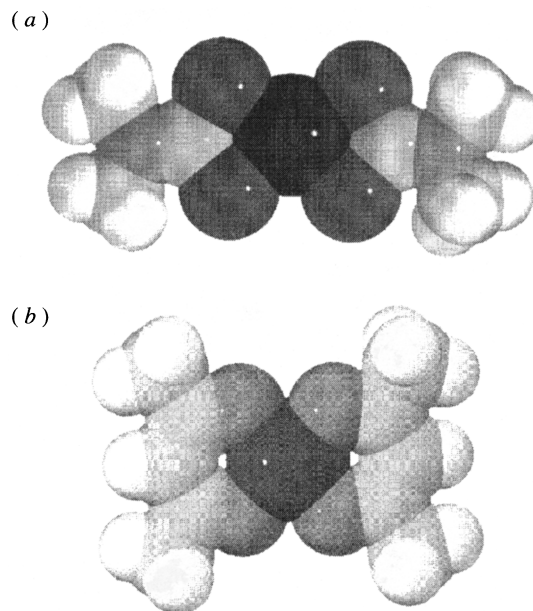


Fig. 5. Space filling models of (a) the  $\text{Co}(\text{dtc})_2$  moiety in  $\text{trans-}[\text{Co}(\text{dtc})_2(\text{PMePh}_2)_2]\text{BF}_4$  (**t-2**) and (b) the  $\text{Co}(\text{acac})_2$  moiety in  $\text{trans-}[\text{Co}(\text{acac})_2(\text{PMePh}_2)_2]\text{PF}_6$ .

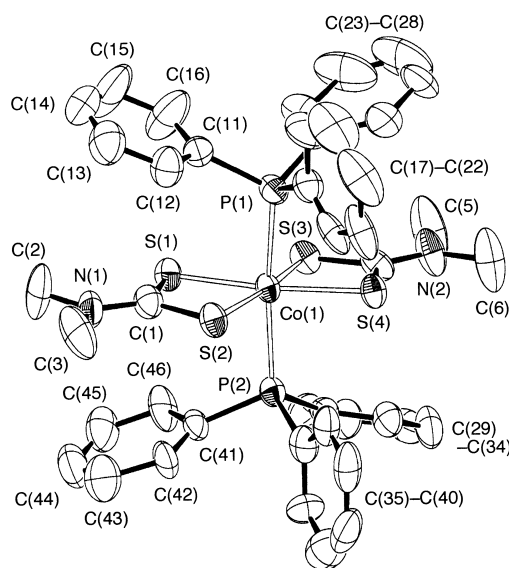


Fig. 6. Perspective drawing (40% probability level; hydrogen atoms are omitted) of one of the complex cations in  $\text{trans-}[\text{Co}(\text{dtc})_2(\text{PPh}_3)_2]\text{BF}_4\cdot\text{H}_2\text{O}$  (**t-3·H2O**).

length in **t-3·H2O** is 2.316 Å, which is extremely shorter (by 0.073 Å) than that in  $\text{trans-}[\text{Co}(\text{acac})_2(\text{PPh}_3)_2]\text{PF}_6$ .<sup>1</sup> As seen from Fig. 7, the  $\text{Co-P}$  bond lengths in **t-1**, **t-2** and **t-3** are linearly correlated to the crystallographic cone angle of  $\text{PMe}_2\text{Ph}$ ,  $\text{PMePh}_2$  and  $\text{PPh}_3$ , although the plot for **t-0** deviates from the linearity due to the strong electronic *trans* influence of  $\text{PMe}_3$  (vide infra). Therefore, what the plots in Fig. 7 indicate is an exceptionally long  $\text{Co-P}$  bond in  $\text{trans-}[\text{Co}(\text{acac})_2(\text{PPh}_3)_2]\text{PF}_6$ . In the previous paper,<sup>1</sup> we have concluded that such long  $\text{Co-P}$  bonds in  $\text{trans-}[\text{Co}(\text{acac})_2(\text{PPh}_3)_2]\text{PF}_6$  result from the severe steric interaction between the equatorial acac and the axial

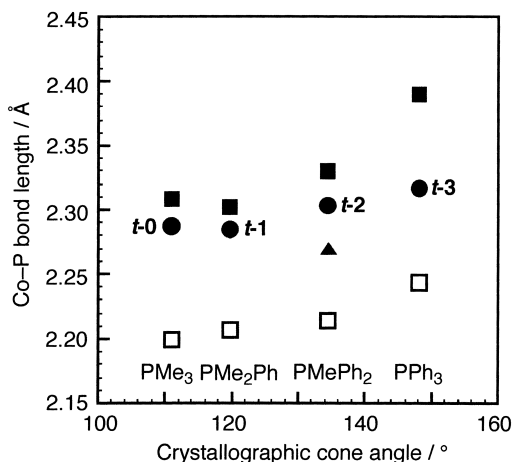


Fig. 7. Comparison of the Co-P bond lengths against the crystallographic cone angles<sup>26</sup> of  $\text{PMe}_{3-n}\text{Ph}_n$ :  $\text{trans}[\text{Co}(\text{dtc})_2(\text{PMe}_{3-n}\text{Ph}_n)_2]^+$  (●);  $\text{trans}[\text{Co}(\text{acac})_2(\text{PMe}_{3-n}\text{Ph}_n)_2]^+$  (■);  $\text{trans}[\text{Co}(\text{acac})_2(\text{PMe}_{3-n}\text{Ph}_n)(\text{H}_2\text{O})]^+$  (□);  $\text{trans}(P,P),\text{cis}(C,C)-[\text{Co}(\text{acac})(\text{CN})_2(\text{PMePh}_2)_2]$  (▲).

$\text{PPh}_3$  ligands in both sides; that is, the steric *trans* influence via equatorial acac ligands, where the steric interaction is mainly associated with the orientation and conformation of three phenyl rings of  $\text{PPh}_3$ . In the present dtc complex, such a steric interaction between the equatorial dtc and the axial  $\text{PPh}_3$  ligands would become less effective because of the compactness and flexibility of dtc coordination, as mentioned above. In fact, one of the phenyl rings of  $\text{PPh}_3$  (and  $\text{PMePh}_2$ ) can orient perpendicularly to fit the cleft of the equatorial  $\text{CoS}_4$  plane, and the other phenyl rings can orient rather freely to minimize the steric interaction. Hence, it is stated that the steric *trans* influence via equatorial dtc ligands is negligible in  $\text{trans}[\text{Co}(\text{dtc})_2(\text{PMe}_{3-n}\text{Ph}_n)_2]\text{BF}_4$ .

A shorter Co-P bond in the related *trans*-bis( $\text{PMePh}_2$ ) type complex has been found in  $\text{trans}(P,P),\text{cis}(C,C)[\text{Co}(\text{acac})(\text{CN})_2(\text{PMePh}_2)_2]$  (2.2698(4) Å; see Fig. 7),<sup>3</sup> which is as stable as the present dtc complexes for hydrolysis. Although the electronic *cis* influence<sup>25</sup> should be taken into consideration for the comparison of their reactivities, it is difficult to evaluate the influence experimentally. However, the Co-P bond lengths are affected by not only the steric but also the electronic influences, so that the length would be a good experimental measure to consider the difference in reactivity, when complexes having the same phosphine are compared. In conclusion, the short Co-P bonds in the dtc complexes are the structural counterpart for the stability toward hydrolysis.

**Spectroscopic Properties.** The absorption spectra of **c-0** and **c-1'**, together with those of  $\text{cis}[\text{Co}(\text{dtc})_2\{\text{P}(\text{OMe})_3\}_2]\text{BF}_4$ <sup>10</sup> and  $[\text{Co}(\text{dtc})_3]$ , are shown in Fig. 8a. The spectra of **c-0** and **c-1'** are very similar to each other in the region up to 34000  $\text{cm}^{-1}$ ; there are two bands with medium intensity around 18000 and 23000  $\text{cm}^{-1}$ , a shoulder feature around 29000  $\text{cm}^{-1}$ , and a very intense band around 32500  $\text{cm}^{-1}$ . The two lowest energy bands are assignable as the first and the second d-d transition ones, respectively, similar to those of the analogous  $\text{cis}[\text{Co}(\text{dtc})_2(\text{P-ligand})_2]^+$  and  $[\text{Co}(\text{dtc})_2(\text{P-P})]^+$  (P-P =  $\text{Me}_2\text{P}(\text{CH}_2)_n\text{PMe}_2$  ( $n = 1$ : dmpm, 2: dmpe, or 3: dmpp) or  $(\text{MeO})_2\text{P}(\text{CH}_2)_2\text{P}(\text{OMe})_2$ ) complexes.<sup>9-11</sup> Due to the lowering

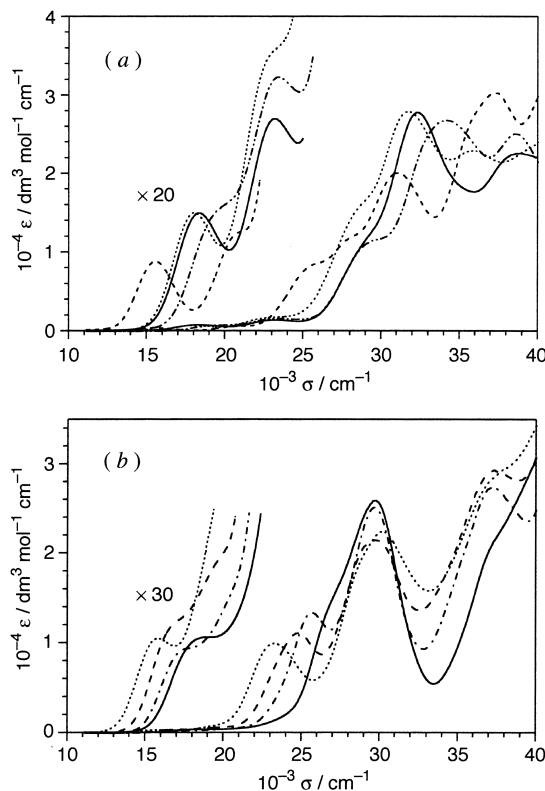


Fig. 8. UV-vis absorption spectra of (a)  $\text{cis}[\text{Co}(\text{dtc})_2(\text{PMe}_3)_2]^+$  (—),  $\text{cis}[\text{Co}(\text{dtc})_2(\text{PMe}_2\text{Ph})_2]^+$  (---),  $\text{cis}[\text{Co}(\text{dtc})_2\{\text{P}(\text{OMe})_3\}_2]^+$  (- · - · -), and  $[\text{Co}(\text{dtc})_3]$  (····); and (b)  $\text{trans}[\text{Co}(\text{dtc})_2(\text{PMe}_{3-n}\text{Ph}_n)_2]^+$  ( $n = 0$  (—); 1 (- · - · -); 2 (---); and 3 (····)) in dichloromethane at room temperature.

molecular symmetry of the complexes from holohedrized  $O_h$  symmetry, the splitting of the d-d transition bands is expected, but the first d-d bands of the complexes (**c-0** and **c-1'**) are found to be as symmetrical as the first d-d band of  $[\text{Co}(\text{dtc})_3]$ . The positions of the first and the second d-d bands of the complexes are estimated by the Gaussian curve fitting analysis, and are listed in Table 5. It is found that the first and the second d-d transition energies of the  $\text{PMe}_3$  complex are slightly higher than those of the  $\text{PMe}_2\text{Ph}$  complex, but are lower than those of the didentate diphosphine (dmpm, dmpe, and dmpp) complexes.<sup>9</sup> It is also interesting to compare these energies to those of the corresponding phosphite ( $\text{P}(\text{OMe})_3$ ,  $\text{P}(\text{OEt})_3$ , and  $\text{P}(\text{OCH}_2)_3\text{CET}$ ) complexes.<sup>10</sup> The first d-d band of the  $\text{PMe}_3$  complex is observed to be lower in energy by 1100  $\text{cm}^{-1}$  than that of the  $\text{P}(\text{OMe})_3$  complex, but the difference in the second d-d transition energy between these complexes is only 400  $\text{cm}^{-1}$  (Table 5). This fact indicates that the interelectronic repulsion parameter,  $B$ , of the  $\text{P}(\text{OMe})_3$  complex is reduced remarkably from that of the  $\text{PMe}_3$  complex. The reduction of  $B$  parameter in the phosphite complex would result from  $\pi$  back-bonding, which is negligible for  $\text{Co}^{\text{III}}$ -phosphine bonds.<sup>7,22</sup>

The absorption spectra of the *trans* series of complexes are shown in Fig. 8b, and the positions of the absorption bands evaluated by the Gaussian curve fitting analysis are listed in Table 5. In the region of 12000–20000  $\text{cm}^{-1}$ , an absorption band or shoulder is observed with the intensity of  $\epsilon \sim 300 \text{ dm}^3$

Table 5. Gaussian Curve Fitting Results for Absorption Spectra of the Complexes,  $10^{-3} \sigma/\text{cm}^{-1}$  ( $\epsilon/\text{dm}^3 \text{mol}^{-1} \text{cm}^{-1}$ )

Complex	d-d Band		CT-band		
<b>c-0</b>	18.33(740.8)	23.31(1340)	29.25(10560)	32.62(24990)	
<b>c-1'</b>	17.91(742.6)	22.96(1716)	28.89(15200)	32.04(21800)	
<b>t-0</b>	17.90(258.1)	22.81(587.0) <sup>a)</sup>	27.38(13540)	30.11(21970)	
<b>t-1</b>	17.17(225.4)	22.12(665.8) <sup>a)</sup>	25.57(12090)	29.70(25120)	
<b>t-2</b>	16.58(354.5)	19.97(580.5)	24.77(10950)	29.63(21750)	
<b>t-3</b>	15.74(342.3)	20.20(868.7) <sup>a)</sup>	23.08(9488)	30.18(22290)	
[Co(dtc) <sub>3</sub> ]	15.50(435.2)	20.62(588.9)	25.87(8437)	27.73(2794)	31.21(19490)
<i>cis</i> -[Co(dtc) <sub>2</sub> - {P(OMe) <sub>3</sub> } <sub>2</sub> BF <sub>4</sub> ]	19.41(704.2)	23.73(1552)	29.03(9840)	34.08(26980)	

a) Very broad shoulder in the observed spectra.

$\text{mol}^{-1} \text{cm}^{-1}$ . This band (or shoulder) is regularly blue-shifted in the order of  $\text{PPh}_3 < \text{PMePh}_2 < \text{PMe}_2\text{Ph} < \text{PMe}_3$ . Previously, for the  $\text{PPh}_3$  complex,<sup>9</sup> we have assigned this band as the degenerate splitting component ( $a^1E_g$ ) of the first d-d transition band under the holohedrized  $D_{2h}$  symmetry, and the same assignment resulted from the analogous acac complexes, *trans*-[Co(acac)<sub>2</sub>( $\text{PMe}_{3-n}\text{Ph}_n$ )<sub>2</sub>]<sup>+</sup>.<sup>1</sup> Interestingly, the transition energies of the dtc and acac complexes are approximately the same; the difference being less than  $300 \text{ cm}^{-1}$ . This fact suggests that the ligand-field strengths of these two series of complexes, *trans*-[Co(dtc)<sub>2</sub>( $\text{PMe}_{3-n}\text{Ph}_n$ )<sub>2</sub>]<sup>+</sup> and *trans*-[Co(acac)<sub>2</sub>( $\text{PMe}_{3-n}\text{Ph}_n$ )<sub>2</sub>]<sup>+</sup>, are nearly the same, when the same phosphine is concerned. There is a very broad shoulder feature observed in the spectra of dtc complexes (Table 5), but we could not assign this transition to either the non-degenerate splitting component ( $^1A_{2g}$ ) or the second d-d transition ones ( $^1B_{2g}$  and  $b^1E_g$ ).

Each complex of *trans*-[Co(dtc)<sub>2</sub>( $\text{PMe}_{3-n}\text{Ph}_n$ )<sub>2</sub>]<sup>+</sup> shows an intense CT band around  $30000 \text{ cm}^{-1}$ . In the lower energy region, there is another CT band, which is regularly blue-shifted as the number of methyl groups of phosphine increased: from  $23080 \text{ cm}^{-1}$  for **t-3** to  $27380 \text{ cm}^{-1}$  for **t-0**. Thus, it seems likely to assign these CT bands to S-to-Co and P-to-Co LMCT transitions, respectively. A P-to-Co LMCT band is also observed for the series of *trans*-[Co(acac)<sub>2</sub>( $\text{PMe}_{3-n}\text{Ph}_n$ )<sub>2</sub>]<sup>+</sup> complexes ( $18970$ ,  $21420$ ,  $22830$ , and  $24640 \text{ cm}^{-1}$  for the  $\text{PPh}_3$ ,  $\text{PMePh}_2$ ,  $\text{PMe}_2\text{Ph}$ , and  $\text{PMe}_3$  complexes, respectively),<sup>1</sup> but the CT transition energy is lower (by more than  $2700 \text{ cm}^{-1}$ ) than the present dtc complex. The P-to-Co LMCT transition energy is estimated by

$$\sigma_{\text{LMCT}} = 30000\{\chi(\text{P-ligand}) - \chi(\text{Co}^{\text{III}})\} + \Delta - 7.6B,$$

where  $\chi(\text{P-ligand})$  and  $\chi(\text{Co}^{\text{III}})$  are the optical electronegativities of P-ligand and  $\text{Co}^{\text{III}}$ .<sup>1,27</sup>

The  $\Delta$  values of the dtc and acac complexes are nearly equal to each other, as suggested in the above. Although it is known that many  $\text{Co}^{\text{III}}$ -dtc complexes show rather large reduction of the interelectronic repulsion,<sup>28</sup> the reduction (expected to be less than  $100 \text{ cm}^{-1}$ ) of  $B$  value alone can not explain the observed large difference in the LMCT transition energy. Therefore, it is indicative of a different optical electronegativity between  $\text{Co}^{\text{III}}(\text{dtc})_2$  and  $\text{Co}^{\text{III}}(\text{acac})_2$  moieties. The fact that the value of  $\chi(\text{Co}^{\text{III}}(\text{dtc})_2)$  obtained by the LMCT transition ener-

gies is smaller than that of  $\chi(\text{Co}^{\text{III}}(\text{acac})_2)$  parallels the electrochemical (reduction potential) data of the related dtc and acac complexes.<sup>7,8,12</sup> The details in electrochemistry of the present complexes will be reported elsewhere, together with those of the related  $\text{P}(\text{OMe})_{3-n}\text{Ph}_n$  complexes.<sup>13</sup>

The data of  $^{31}\text{P}$  and  $^{59}\text{Co}$  NMR chemical shifts of the complexes are also given in Table 2. Except for **t-3**, all of the complexes gave a broad  $^{59}\text{Co}$  resonance in the region of  $\delta$  3000–4000, but these values are very different from those of the corresponding acac complexes ( $\delta$  12200–13000).<sup>1</sup> Because at least the  $a^1E_g$  transition energies of the dtc and acac complexes are nearly equal, the difference in the  $^{59}\text{Co}$  NMR chemical shifts may indicate a large difference in reduction parameter,  $\alpha$ ,<sup>1,29</sup> between these two series of complexes, but the details are still unknown at present.

## Conclusion

The compactness and flexibility of dtc coordination have given rise to remarkable differences in the structures of the mixed-ligand dtc-phosphine cobalt(III) complexes from those of the corresponding acac-phosphine complexes. The most intriguing differences have been found in the structures of *trans*-[Co(dtc)<sub>2</sub>( $\text{PMePh}_2$  or  $\text{PPh}_3$ )<sub>2</sub>]<sup>+</sup>BF<sub>4</sub> (**t-2** or **t-3**) and *trans*-[Co(acac)<sub>2</sub>( $\text{PMePh}_2$  or  $\text{PPh}_3$ )<sub>2</sub>]<sup>+</sup>PF<sub>6</sub>,<sup>1,3</sup> which contain sterically rather bulky phosphines. While all complexes of *trans*-[Co(acac)<sub>2</sub>( $\text{PMe}_{3-n}\text{Ph}_n$ )<sub>2</sub>]<sup>+</sup> and *trans*-[Co(dtc)<sub>2</sub>( $\text{PMe}_3$  or  $\text{PMe}_2\text{Ph}_2$ )<sub>2</sub>]<sup>+</sup> have crystallographically imposed  $C_i$  molecular symmetry with the inversion center at the Co atom, the complexes of *trans*-[Co(dtc)<sub>2</sub>( $\text{PMePh}_2$  or  $\text{PPh}_3$ )<sub>2</sub>]<sup>+</sup> have (crystallographically imposed or pseudo)  $C_2$  molecular symmetry, where the size of two clefts in the equatorial Co(dtc)<sub>2</sub> plane is remarkably different (Fig. 5a), as exemplified by two angles of S(1)–Co–S(1') and S(2)–Co–S(2') for **t-2**. Toward the larger cleft, one of the phenyl rings of  $\text{PMePh}_2$  or  $\text{PPh}_3$  is oriented perpendicularly to minimize the steric interaction between the equatorial dtc and the axial phosphine ligands (Fig. 4b). Such a perpendicular orientation of phenyl ring would be prohibited for the bis(acac) complexes because of the larger steric requirement of acac, so that a strong steric *trans* influence via the equatorial acac ligands for the elongation of mutually *trans* Co–P bonds would be expected, especially for the  $\text{PPh}_3$  complex. In contrast, the steric *trans* influence via the equatorial dtc ligands would, therefore, be negligibly weak. This is reflected in the Co–P bond lengths in *trans*-[Co(dtc)<sub>2</sub>( $\text{PMe}_{3-n}$ -

$\text{Ph}_n)_2]^+$  being shorter than those in the corresponding *trans*- $[\text{Co}(\text{acac})_2(\text{PMe}_{3-n}\text{Ph}_n)_2]^+$ ; also the shorter Co–P bonds observed can interpret the stability of the dtc complexes toward hydrolysis.

It has also been found that the Co–S bond lengths in the dtc–phosphine complexes vary with two effects: (1) the intramolecular  $\pi$ – $\pi$  stacking interaction between the dtc plane and the phenyl ring of phosphine, and (2) the electronic *trans* influence of the phosphine. The  $\pi$ – $\pi$  stacking interaction makes the interacting Co–S bond length shorter, as illustrated most clearly in the structure of *trans*- $[\text{Co}(\text{dtc})_2(\text{PMe}_2\text{Ph})_2]^+$ . Comparison of the Co–S bond lengths which do not have the stacking interaction in *cis*- $[\text{Co}(\text{dtc})_2(\text{PMe}_3, \text{PMe}_2\text{Ph}, \text{or } \text{P}(\text{OCH}_2)_3\text{CEt})_2]^+$  gives the order of the strength of the electronic *trans* influence as  $\text{PMe}_3 > \text{PMe}_2\text{Ph} > \text{P}(\text{OCH}_2)_3\text{CEt}$ , which is in accordance with the order of their  $\sigma$ -donicity. In contrast, the first d–d transition energies of *cis*- $[\text{Co}(\text{dtc})_2(\text{PMe}_3, \text{PMe}_2\text{Ph}, \text{or } \text{P}(\text{OMe})_3)_2]^+$  do not follow the order of  $\sigma$ -donicity of the P-ligands. The first d–d transition band of the  $\text{PMe}_3$  complex is observed at an energy lower by  $1100 \text{ cm}^{-1}$  than that of the  $\text{P}(\text{OMe})_3$  complex, but the difference in energy of the second d–d band between these complexes is only  $400 \text{ cm}^{-1}$ . This indicates that the interelectronic repulsion parameter,  $B$ , in the  $\text{P}(\text{OMe})_3$  complex ( $B = 270 \text{ cm}^{-1}$ ) is much reduced from that in the  $\text{PMe}_3$  complex ( $311 \text{ cm}^{-1}$ ).

The authors wish to thank Prof. Shigeru Ohba (Keio University) and Mr. Seiji Adachi (Osaka University) for the structural analysis of compound *t*-2 and measurements of  $^{31}\text{P}$  and  $^{59}\text{Co}$  NMR spectra, respectively.

## References

- 1 T. Suzuki, S. Kaizaki, and K. Kashiwabara, *Inorg. Chim. Acta*, **298**, 131 (2000).
- 2 T. Suzuki, K. Kashiwabara, M. Kita, J. Fujita, and S. Kaizaki, *Inorg. Chim. Acta*, **281**, 77 (1998).
- 3 K. Kashiwabara, M. Kita, H. Masuda, S. Kurachi, and S. Ohba, *Bull. Chem. Soc. Jpn.*, **68**, 883 (1995).
- 4 K. Katoh, H. Sugiura, K. Kashiwabara, and J. Fujita, *Bull. Chem. Soc. Jpn.*, **57**, 3580 (1984); K. Kashiwabara, K. Katoh, T. Ohishi, J. Fujita, and M. Shibata, *Bull. Chem. Soc. Jpn.*, **55**, 149 (1982).
- 5 S. Hayakawa, H. Nishikawa, K. Kashiwabara, and M. Shibata, *Bull. Chem. Soc. Jpn.*, **54**, 3593 (1981).
- 6 M. Kita, K. Kashiwabara, and J. Fujita, *Bull. Chem. Soc. Jpn.*, **61**, 3187 (1988); M. Kita, K. Nemoto, K. Kashiwabara, J. Fujita, M. Goto, T. Miyamoto, and S. Ohba, *Bull. Chem. Soc. Jpn.*, **66**, 1687 (1993); M. Takata, K. Kashiwabara, H. Ito, T. Ito, and J. Fujita, *Bull. Chem. Soc. Jpn.*, **58**, 2247 (1985); M. Atoh, I. Kinoshita, K. Kashiwabara, and J. Fujita, *Bull. Chem. Soc. Jpn.*, **55**, 3179 (1982).
- 7 M. Kita and K. Kashiwabara, *Polyhedron*, **16**, 2771 (1997).
- 8 M. Adachi, M. Kita, K. Kashiwabara, J. Fujita, N. Iitaka, S. Kurachi, and S. Ohba, *Bull. Chem. Soc. Jpn.*, **65**, 2037 (1992).
- 9 M. Kita, A. Okuyama, K. Kashiwabara, and J. Fujita, *Bull. Chem. Soc. Jpn.*, **63**, 1994 (1990).
- 10 H. Matsui, M. Kita, K. Kashiwabara, and J. Fujita, *Bull. Chem. Soc. Jpn.*, **66**, 1140 (1993).
- 11 M. Kita, M. Okuno, K. Kashiwabara, and J. Fujita, *Bull. Chem. Soc. Jpn.*, **65**, 3042 (1992).
- 12 M. Okuno, M. Kita, K. Kashiwabara, and J. Fujita, *Chem. Lett.*, **1989**, 1643.
- 13 K. Kashiwabara, T. Suzuki et al., to be published; S. Kashiwabara, K. Kashiwabara, M. Kita, and J. Fujita, The 43rd Symposium on Coordination Chemistry of Japan, Sendai (1993), Abstract 3A07.
- 14 T. Suzuki, S. Iwatsuki, H. D. Takagi, and K. Kashiwabara, *Chem. Lett.*, **2001**, 1068.
- 15 H. Iwasaki and K. Kobayashi, *Acta Crystallogr., Sect. B*, **36**, 1657 (1980).
- 16 A. Yamasaki, *J. Coord. Chem.*, **24**, 211 (1991).
- 17 P. Coppens, L. Leiserowitz, and D. Rabinovich, *Acta Crystallogr.*, **18**, 1035 (1965).
- 18 A. C. T. North, D. C. Phillips, and F. S. Mathews, *Acta Crystallogr., Sect. A*, **24**, 351 (1968).
- 19 G. M. Sheldrick, *Acta Crystallogr., Sect. A*, **46**, 467 (1990).
- 20 G. M. Sheldrick, SHELXL97, University of Göttingen, Germany (1997).
- 21 Molecular Structure Corporation and Rigaku Co. Ltd., TeXsan, Single crystal structure analysis software, ver. 1.9, The Woodlands, TX, USA and Akishima, Tokyo, Japan (1998).
- 22 H.-Y. Liu, K. Eriks, A. Prock, and W. P. Giering, *Organometallics*, **9**, 1758 (1990); Md. M. Rahman, H.-Y. Liu, K. Eriks, A. Prock, and W. P. Giering, *Organometallics*, **8**, 1 (1989).
- 23 C. A. Tolman, *Chem. Rev.*, **77**, 313 (1977).
- 24 For this comparison, only Co–P(2) =  $2.2637(7) \text{ \AA}$  of *c*-1' is used as the relevant Co–P bond length in the *cis*-isomer, because the  $\text{PMe}_2\text{Ph}$  ligands in *t*-1 have a stacking interaction with dtc as the P(2)Me<sub>2</sub>Ph in *c*-1'.
- 25 N. Bresciani-Pahor, M. Forcolin, L. G. Marzilli, L. Randaccio, M. F. Summers, and P. J. Toscano, *Coord. Chem. Rev.*, **63**, 1 (1985); N. Bresciani-Pahor, M. Calligaris, G. Nordin, and L. Randaccio, *J. Chem. Soc., Dalton Trans.*, **1982**, 2549.
- 26 T. E. Müller and D. M. P. Mingos, *Transition Met. Chem.*, **20**, 533 (1995).
- 27 A. B. P. Lever, "Inorganic Electronic Spectroscopy," 2nd Ed., Elsevier, Amsterdam (1984), Chap. 5.
- 28 T. Ohishi, K. Kashiwabara, and J. Fujita, *Bull. Chem. Soc. Jpn.*, **60**, 583 (1987).
- 29 Y. Shimura, *Bull. Chem. Soc. Jpn.*, **61**, 693 (1988).